On the Characterization of the Main Phase in K_x*p*-Terphenyl and its Largest Congener K_xPoly-*p*-Phenylene. A Report of their Magnetic and Electric Properties

Manuel Carrera,[1] James L. McDonald,[1] Carlos Untiedt,[2] Mar García-Hernández,[3] Federico Mompean,[3] José Antonio Vergés,[4] and Albert Guijarro.[1]

[1]Departamento de Química Orgánica and Instituto Universitario de Síntesis Orgánica, and

[2]Departamento de Física Aplicada,

Campus de San Vicente del Raspeig, Universidad de Alicante, Apdo. 99, 03080 Alicante, Spain.

[3]Departamento de Materiales para Tecnologías de la Información, and

[4]Departamento de Teoría y Simulación de Materiales,

Instituto de Ciencia de Materiales de Madrid (CSIC), Cantoblanco, 28049, Madrid, Spain

ABSTRACT

The report of the Meissner effect in annealed samples of K_3Tp (Tp = *p*-terphenyl) above 120 K has raised the interest in this deceptively simple material concerning superconductivity. We have investigated the structural integrity of the Tp framework in annealed samples of K_xTp at increasing processing time and temperature *T*. Our experimental studies show that both K_2Tp and K_3Tp mixing stoichiometries have identical Raman (solid state) and UV-vis (DME solution) spectra, being consistent with the molecular dianion by DFT and TDDFT simulations. Magnetization vs. *T* plots show no signs of superconductivity, and neither do conductance vs. *T* plots. Searching for potentially active minor byproducts formed during thermal processing, the role of K-doped poly-*p*-phenylene (K_xPPP) has been examined but it does not seem to explain the reported effects either. Further efforts are needed to explain the nature of this elusive phenomenon.

1. INTRODUCTION

Potassium doped *p*-terphenyl with the stoichiometry of K_3*p*-terphenyl (K_3Tp) has attracted much attention in the area of organic superconductors after the report of an ongoing series of experiments by X.-J. Chen and collaborators in which an apparent transition to the superconducting phase occurred at an ever increasing range of critical temperatures, T_c = 7.2 K,[1] 43 K,[2] and even 123 K,[3] all for the same compound. Unfortunately, only a very small fraction of

[1] R.-S. Wang, Y. Gao, Z.-B. Huang, X.-J. Chen, Superconductivity in p-Terphenyl. 2017, arXiv:1703.05803. http://lanl.arxiv.org/abs/1703.05803 (accessed Dec. 11, 2018).

[2] R.-S. Wang, Y. Gao, Z.-B. Huang, X.-J. Chen, Superconductivity at 43 K in a Single C-C Bond Linked Terphenyl. 2017, arXiv:1703.05804. http://lanl.arxiv.org/abs/1703.05804 (accessed Dec. 11, 2018).

the annealed reaction crude could account for the observed Meissner effect, which is very weak in these materials. The difficulties associated with the observation of a potentially superconducting phase under these circumstances are many; even worsened by a presumably complex non-homogeneous nature of the samples, that are devoid of suitable purification techniques and have an inherent extreme degradability to air/moisture. In spite of that, sporadic findings have appeared corroborating a magnetic behavior similar to that observed in K_3Tp at temperatures near 120 K, again only for a very small fraction of the analyzed sample.[4,5] Whether this corresponds to a superconducting signature or not is an issue that remains to be addressed. However, the significance of these findings calls for a careful analysis of the current species present in the K_3Tp samples, as well as a study of the potential minor byproducts that could account for the reported magnetic properties. Current structural knowledge of these materials is scarce. A limited crystallinity of the bulk material prevents it to be properly analyzed by standard X-ray diffraction (XRD) techniques, so a clear structural picture is yet obscure from the experimental side. There are attempts to model the crystal structure using computational methods of solid-state DFT,[6] but in general fail to reproduce the powder XRD pattern.[7] In this study, we

---

[3] R.-S. Wang, Y. Gao, Z.-B. Huang, X.-J. Chen, Superconductivity Above 120 Kelvin in a Chain Link Molecule. 2017, arXiv:1703.06641. http://lanl.arxiv.org/abs/1703.06641 (accessed Dec. 11, 2018).

[4] W. Liu, H. Lin, R. Kang, X. Zhu, Y. Zhang, S. Zheng, H.-H. Wen, Magnetization of potassium-doped p-terphenyl and p-quaterphenyl by high-pressure synthesis, *Phys. Rev. B*, **2017**, *96*, 224501.

[5] P. Neha, A. Bhardwaj, Vikrant Sahu, S. Patnaik, Facile synthesis of potassium intercalated p-terphenyl and signatures of a possible high Tc phase, *Physica C*, **2018**, 554, 1–7.

[6] X.-W. Yan, Z. Huang, M. Gao, C. Zhang, Stable Structural Phase of Potassium-Doped p-Terphenyl and Its Semiconducting State, *J. Phys. Chem. C*, Just Accepted Manuscript. DOI: 10.1021/acs.jpcc.8b10114.

undertake the characterization of a range of K_xTp samples obtained under different experimental conditions, as well as potentially related materials that might have evolved from them by thermal processing, hoping to identify the source of the reported magnetic properties. In our quest, the role of the largest possible congener, $K_x$poly-*p*-phenylene (K_xPPP), which is the maximum attainable size within the class, has been examined in detail. With all these materials in hand, the magnetic and electrical conduction properties were determined and observed divergences with published studies discussed.

2. THERMAL RESILIENCE OF K_xTp MIXTURES

Our first concern was with the thermal stability of the molecular *p*-terphenyl backbone after reaction with potassium under the typical annealing conditions and times,[3] as well as under a variety of milder reaction conditions. The reaction of Tp with K proceeds smoothly above the melting point of potassium (63.7ºC), although it also occurs at lower temperatures by grinding. The stoichiometry was set to 3:1. The reaction at 100ºC is completed within minutes provided that the mixing is efficient, affording a black powder that has no remains of Tp by XRD and Raman, but shows some unreacted K by XRD using Cu K_α radiation (cubic cell: a = 5.25 Å) unnoticeable by simple visual examination. This black compound was annealed during increasing periods of time, and at different temperatures in different runs. The samples were then reoxidized back to Tp by exposure to air and quantitatively analyzed (see experimental section). The recovered amount of the intact hydrocarbon vs. time and vs. temperature is represented in Figure 1. At 100ºC during 24h the amount of recovered Tp is

---

[7] Zhong, G.-H.; Wang, X.-H.; Wang, R.-S.; Han, J.-X.; Zhang, C.; Chen, X.-J.; Lin, H.-Q. Structural and Bonding Characteristics of Potassium-Doped p-Terphenyl Superconductors, *J. Phys. Chem. C* **2018**, *122*, 3801−3808.

nearly quantitative (98%), and only a slow decrease in the percent of recovered Tp is manifested upon prolonged annealing times (98, 96, 89, 88, 80 and 78% recovered at 24, 40, 72, 102, 144 and 178 h, respectively). The effect of the annealing temperature is more severe to the degradation. At 250ºC during 24h about one third of the starting Tp has been converted into other byproducts, increasing to two thirds in 72h (68 %, 34% recovered at 24 h and 72 h, respectively).

The structural integrity of the *p*-terphenyl backbone seems therefore to be compromised, but only under intense thermal treatment. Concerning those byproducts, mass spectroscopy by direct insertion probe (DIP-MS) allowed us to examine some of the volatile compounds other than Tp after the recovery process in harshly annealed samples. Small amounts of a dimer of molecular weight M^+ = 458.2, as well as much smaller amounts of other oligomers of M^+ = 534.2, 610.3 and 686.3, all consistent with the generic formula $H(C_6H_4)_nH$, with n= 6,7, 8 and 9 were detected. Still, most of the remaining material after Tp extraction is highly insoluble and non-volatile, indicating an extensive thermal degradative polymerization. In Scheme 1, a potential oligo and polymerization pathway occurring between two adjacent cells in the solid state is proposed. Thermally promoted intercell coupling between Tp anions creates dihydro intermediates that may recover π conjugation after KH elimination giving rise to intercalated oligo-*p*-phenylenes. Further processing by the same mechanisms would render K-intercalated poly-*p*-phenylenes. In this simplified model of polymerization, starting from an initial stoichiometry of K_3Tp, a final intercalated poly-*p*-phenylene of generic composition $[K(C_6H_4)_3]_n$ would be achieved. We have observed the presence of KH (cubic cell: a = 5.71 Å) by XRD using Cu K_α radiation in samples intensely annealed (250ºC/72 h). KH is however absent in samples mildly annealed (100ºC/24 h or 70ºC/24 h in cyclohexane)

of similar visual aspect. The presence of KH can be identified in the XRD pattern of annealed K_3Tp samples reported by other groups.[4]

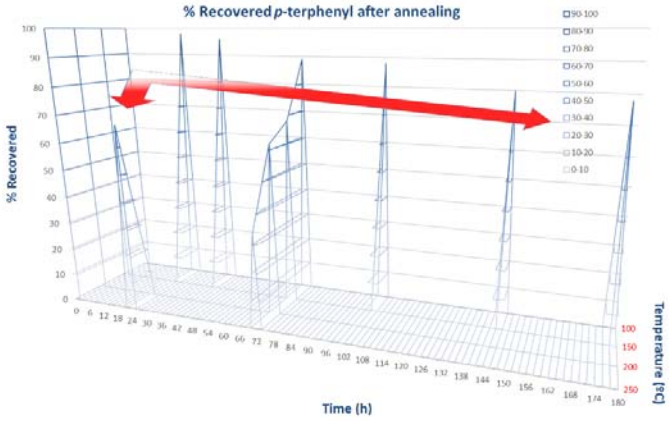

Figure 1. A graphic of chemical recovery of Tp from K_3Tp by air oxidation against annealing time (h) and temperature (ºC). The slopped red arrows emphasize a slow decay in the percent of intact recovered starting material after increasing processing time, and a more intense decay by increasing the processing temperature.

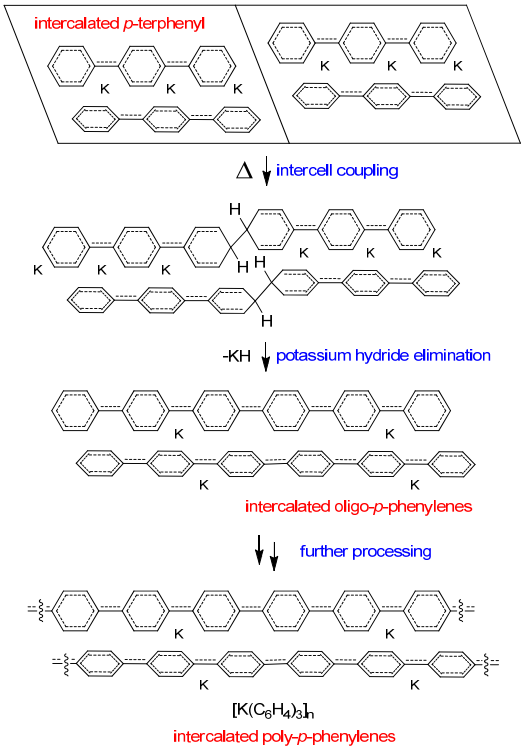

Scheme 1. From the top and downwards, starting from a herringbone K-intercalated *p*-terphenyl solid phase, a mechanism for thermal oligo and polymerization of K_xTp involving coupling between the unsubstituted *para*- positions and concomitant KH elimination to regain conjugation is shown. Starting from an initial mixing ratio of K_3Tp, an ideal final intercalated poly-*p*-phenylene of generic composition $[K(C_6H_4)_3]_n$ would be generated.

3. RAMAN CHARACTERIZATION OF K_xTp SAMPLES

We have examined the Raman spectra of different powder samples of formal composition K_xTp, with x= 0, 1, 2, 3 or higher (up to 6), annealed under mild conditions (100ºC/24h neat, or 70ºC/24h in cyclohexane).[8] Regardless of the initial mixing ratios, all the samples with

[8] Former Raman studies of *p*-terphenyl as well as *p*-terphenyl anions in solution are described in the literature: a) K. Honda, Y Furukawa, Conformational analysis of p-terphenyl by vibrational

stoichiometry x≥2 display the same Raman experimental spectrum, which is coincident with K_2Tp (excitatory frequency 532 nm). A representative spectrum of K_2Tp is reported in Figure 2, while the undoped hydrocarbon Tp can be found in Figure 3. In the case of x=1, a mixture of the free hydrocarbon and dipotassium salt is unveiled by using different excitatory laser frequencies (532 and 633 nm). Assignment of experimental spectrum was done by examining the molecular vibrational modes of the different calculated anions of *p*-terphenyl^{-x} followed by regression analysis against the experimental peaks. The largest 9-10 peaks in the 500-1700 cm^{-1} region of the spectra were included in the analysis. By far, the best fitting (R^2= 0.9989) is found for *p*-terphenyl dianion (Tp^{-2}) (Figure 2, bottom panel). The totally symmetric vibrational modes A_g of the D_{2h} group account for the majority of the active modes in the dianion and neutral Tp, with a few B_{1g}, B_{2g} and B_{3g} modes among some of the minor peaks. Upon reaction with potassium, two important and revealing changes in the spectrum of Tp can be highlighted. It has been colored in red the ν_{57} mode of the neutral compound (exp. peak 11 in Figure 3) and ν_{64} of the dianion (exp. peak 9 in Figure 2), both corresponding to the same 9th A_g vibrational mode in each species. There is a remarkable shift to higher energies of $\Delta\nu$ (Tp $\nu_{57} \rightarrow Tp^{-2}$ ν_{64}) = 72 cm^{-1} clearly seen in the spectrum. The calculated atomic displacements for these two important A_g modes are displayed in Figure 4. They correspond mainly to the inter-ring C-C symmetric stretching vibration along with some symmetric C-H bending. Uptake of electrons provokes a change in bond orders consistent with a strengthening of the inter-ring bonds (quinoid-like structure) in comparison to the neutral hydrocarbon (benzenoid structure). Another subtler change highlighted in green

---

spectroscopy and density functional theory calculations *J. Mol. Struct.* **2005**, *735-736*, 11-19. b) Y Furukawa, H. Ohtsuka, M. Tasumi, Raman studies of polarons and bipolarons in sodium-doped poli-p-phenylene, *Synth. Met.* **1993**, *55-57*, 516-523.

is the increase of the intensity of the symmetric C-H bending mode ν_{69} of the neutral form (exp. small peak 12 in Figure 3) into ν_{70} in the dianion form (exp. peak 9 in Figure 2), both corresponding to the same 10th A_g vibrational mode in each species. This change occurs with an expected shift to lower energies likely due to a non-negligible population of the antibonding C-H orbitals, which likely causes an $\Delta\nu$ ($\nu_{69} \rightarrow \nu_{70}$) = −29 cm^{-1} and an actual large increment of the fully symmetric quadratic component of the molecular polarizability. A similar reasoning can be given for ν_{19} of the dianion (exp. peak 3 in Figure 2), tentatively assigned to the 4th B_{2g} mode which is almost absent in the neutral hydrocarbon.

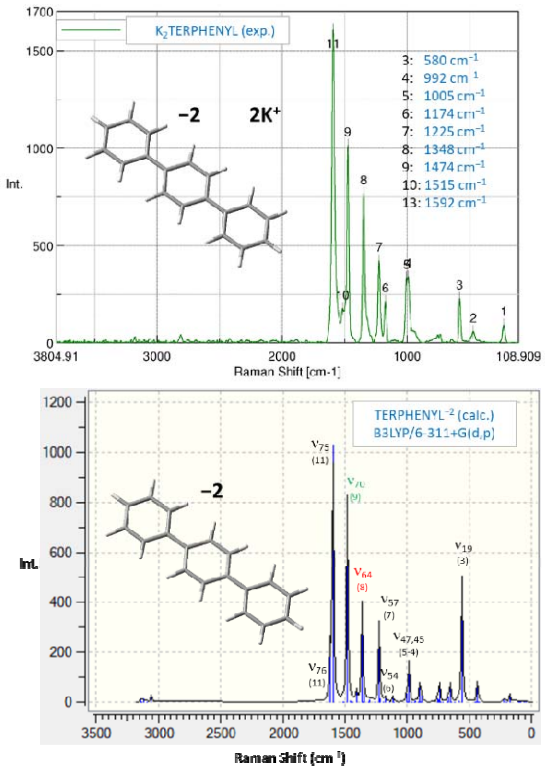

Figure 2. On the top, the experimental full Raman spectrum of K_2Tp powder, found to be identical for all mixing stoichiometries of K_xTp with x≥2 (excitatory frequency 532 nm). On the bottom, the calculated spectrum of Tp^{-2} with the corresponding assignment of the principal

active modes (ν_i) and correspondence to the experimental peaks above (*n*). Highlighted in red and green are two of the peaks showing the most noticeable spectroscopic changes upon K reduction of Tp (see Figure 3 and 4).

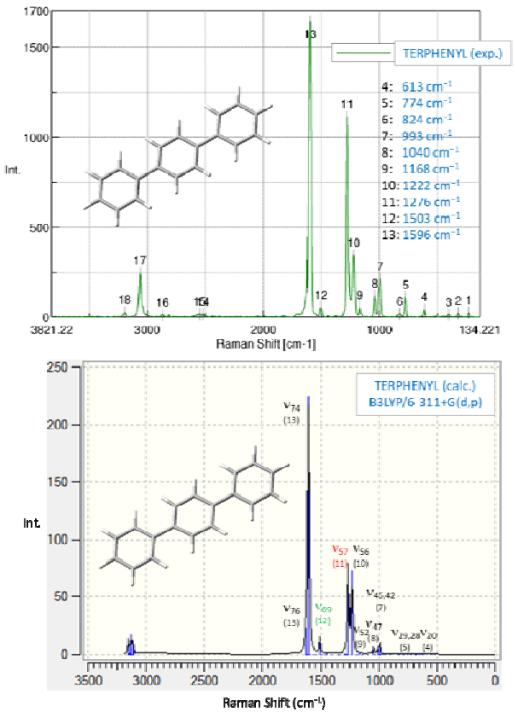

Figure 3. On the top, the experimental full Raman spectrum of Tp powder (excitatory frequency 532 nm). On the bottom, the calculated spectrum of neutral Tp with the corresponding assignment of the principal active modes (ν_i) and correspondence to the experimental peaks above. Highlighted in red and green and corresponding to those in Figure 2 are the two peaks that show the most noticeable spectroscopic changes upon K reduction of Tp (see Figure 2 and 4).

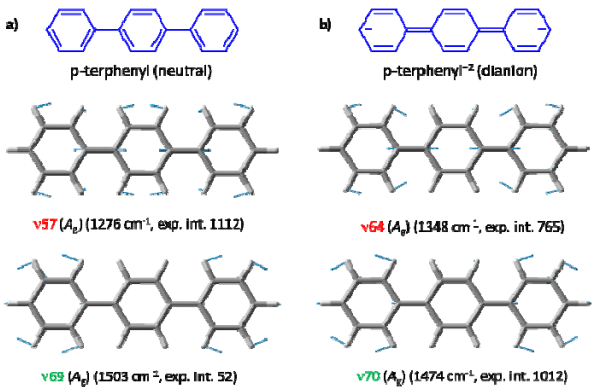

Figure 4. Representative resonance structures of a) Tp, and b) Tp^{-2}, and important vibrational modes disclosing structural changes during the reduction process. Upon electron uptake, the benzenoid form a) turns into a quinoid form b) with a concomitant increase in the inter-ring bond orders and its associated C-C stretching vibrational energy, which can be tracked to the 9th A_g vibrational mode in both species, $\nu_{57} \rightarrow \nu_{64}$, respectively. Another observed effect is an important increase of the intensity of the symmetric C-H bending of the 10th A_g vibrational mode, $\nu_{69} \rightarrow \nu_{70}$, respectively. A full account of the calculated vibrational modes can be found in the SI.

4. RAMAN CHARACTERIZATION OF POTASSIUM INTERCALATED POLY-*p*-PHENYLENE (K_xPPP)

Turning now to poly-*p*-phenylene (or PPP = $(p\text{-}C_6H_4)_n$), we have synthesized linear PPP polymer by means of the Yamamoto procedure, a nickel(II) mediated Kumada-Corriu homocoupling of the Grignard reagent derived from 1,4-dibromobenzene, which was used as a starting material.[9] Strictly linear PPP obtained in this way is a yellow highly insoluble powder

[9] a) T. Yamamoto, A. Yamamoto, A novel type of polycondensation of polyhalogenated organic aromatic compounds producing thermostable polyphenylene type polymers promoted by nickel complex, *Chem. Lett.* **1977**, *6*, 353-356. b) R. S. Sprick, B. Bonillo, R. Clowes, P. Guiglion, N. J. Brownbill, B. J. Slater, F. Blanc., M. A. Zwijnenburg, D. J. Adams, A. I. Cooper, Visible-light-

structurally more regular than an easily available yet randomly branched (or even partially fused) polymer generally obtained by the Kovacic method, an oxidative cationic polymerization process starting from benzene, of brown color (Scheme 2).[10]

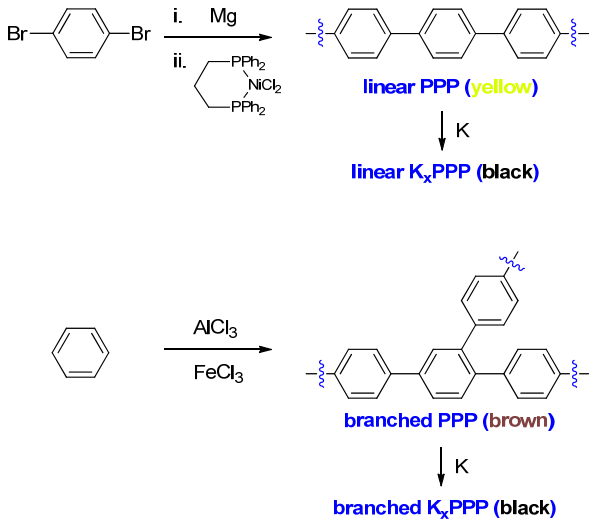

Scheme 2. Poly-*p*-phenylene was synthesized preserving the linear structure (Yamamoto's PPP, yellow), and less regularly allowing for branching (Kovacic's PPP, brown). Both readily uptake K by mild annealing affording black K_xPPP.

There are no reported studies of alkali metal intercalated PPP (i.e. K_xPPP) obtained by annealing in the solid state, although doping in solution using potassium in THF in the presence of naphthalene as electron carrier is known since the 1980s.[11] In those studies, which were

---

driven hydrogen evolution using planarized conjugated polymer photocatalysts, *Angew. Chem.* **2016**, *128*, 1824-1828.

[10] P. Kovacic, A. Kyriakis, Polymerization of benzene to p-polyphenyl, *Tetrahedron Lett*. **1962**, *3*, 467-469.

[11] L . W. Shacklette, R. R. Chance, D. M. Ivory, G. G. Miller, R. H. Baughman, Electrical and optical properties of highly conducting charge-transfer complexes of poly(p-phenylene), *Synth. Met.* **1980**, *1*, 307-320.

performed using PPP obtained by the oxidative cationic polymerization route, it was established that the maximum donor dopant level was approximately one potassium atom for every two-monomer units. Later, the same doping procedure in THF solution but using linear PPP and sodium instead of potassium resulted in doped polymers that were studied by Raman spectroscopy, identifying polaronic and bipolaronic bands.[12] We have evaluated the K uptake ability of the linear polymer by annealing, studying the evolution of the Raman spectra as the K load was increased, from ratios (*p*-C_6H_4)/K = 3/1, 2/1, 3/2, 1/1 and 1/2, as well as quasi-stoichiometric amounts 2/0.9 and 2/1.1. Our results reveal that the maximum doping level is also achieved at the 2/1 ratio, consistent with the approximate formula $[K(C_6H_4)_2]_n$. Higher potassium loads afford only indistinguishable Raman spectra. Concerning branched K_xPPP, it shows intense fluorescent backgrounds when visible laser wavelengths were used for Raman excitation, difficulting the analysis. The problem is minimized in linear PPP by increasing the laser wavelength (632 nm), and can be overcome by applying background subtraction. Linear PPP shows three strong bands at 1598 (1), 1285 (2) and 1225 cm^{-1} (3) (Figure 5, bottom), which have been assigned to three fully symmetric A_g modes assuming a PPP model of D_{2h} symmetry.[13] Upon reaction with an excess of potassium, bands 1 and 3 show little change in their frequencies, becoming bands 10 and 6 in K_xPPP, respectively (Figure 5, top), identified by comparison of the atomic displacements of the corresponding A_g vibrational modes in the calculated models. By contrast, the band 2 at 1285 cm^{-1} turns into band 8 at 1352 cm^{-1}, an upshift of $\Delta\nu$ = 67 cm^{-1} to

---

[12] Y Furukawa, H. Ohtsuka, M. Tasumi, Raman studies of polarons and bipolarons in sodium-doped poli-p-phenylene, *Synth. Met.* **1993**, *55-57*, 516-523.

[13] S. Krichene, J. P. Buisson, S. Lefrant, Interpretation of vibrational studies in phenyl compounds: from oligophenylenes to polyparaphenylene, *Synth. Met.* **1987**, *17*, 589-594, and references therein.

higher energies characteristic from a bipolaronic band that resembles also that displayed by *p*-terphenyl, q.v. This characteristic band corresponds again to the A_g inter-ring C-C symmetric stretching vibration coupled with some symmetric C-H bending, reflecting a higher inter-ring π bond order consistent with the structural changes underwent by extensive electron doping in K_xPPP. Some new bands such as 9 and 5 also develop as a consequence of an increase in the intensity of two A_g symmetric C-H bending modes barely visible in neutral PPP, again similar to what happened in Tp. Bands 4 and 3 also see their intensity significantly increased respect to PPP. Similar shifts in the main Raman peaks upon Na doping have been discussed elsewere,[12] and their underlying nature can be understood by examining the assignment of the Raman spectrum to the calculated vibrational modes in PPP,[14] as well as to the series of neutral and charged oligophenylenes of increasing length, successfully employed as models of polarons and bipolarons.[15] Figure 5 collects the experimental spectra of undoped and heavily doped K_xPPP, better represented as $[K(C_6H_4)_2]_n$ from our studies. For lower K loads, a Raman spectrum that could be interpreted as a polymer with mixed regions of bipolaronic (dianionic), polaronic (monoanions) and benzenoid (neutral) structure is observed (see SI for *p*-C_6H_4/K = 3/1).

---

[14] A) G. Zannoni, G. Zerbi, Lattice dynamics and vibrational spectra of undoped and doped polyparaphenylene, *J. Chem. Phys.* **1985**, *82*, 31-38. B) R. B. Capaz, M. J. Caldas, Ab initio calculations of structural and dynamical properties of poly(p-phenylene) and poly(p-phenylene vinylene), *Phys. Rev. B* **2003**, *67*, 205205-1-9.

[15] K. Honda, Y. Furukawa, K. Furuya, H. Torii, M. Tasumi, Density functional theory study on the Raman spectra of negative polarons and negative bipolarons in Na-doped poly(p-phenylene) *J. Phys. Chem. A* **2002**, *106*, 3587-3592.

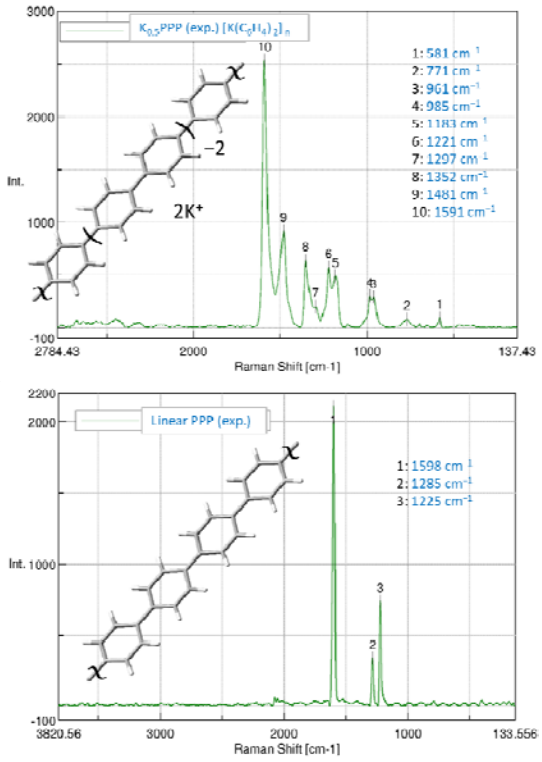

Figure 5. On the top, the experimental full Raman spectrum of K_xPPP powder (excitatory frequency 632 nm), found to be identical for all mixing stoichiometries of K_xPPP with $x \geq 2$ and represented hence as $[K(C_6H_4)_2]_n$. The insert drawing emphasizes the bipolaronic structure of the compound. On the bottom, the full experimental spectrum of linear PPP (excitatory frequency 532 nm).

5. UV-vis CHARACTERIZATION OF K_xTp SAMPLES

The powder nature and intense black color of the samples makes difficult to register what would be an otherwise very informative electronic spectrum of the intercalated material. Instead, we have taken into solution of 1,2-dimethoxyethane (DME) different samples of formal composition K_xTp, with x = 2, 3 or higher annealed under mild conditions (100ºC/24h neat, or 70ºC/24h in cyclohexane) and recorded the UV-vis spectra using a flow cell under a strictly inert

environment. Again, regardless of the initial mixing ratios, all the samples with stoichiometry x = 2, 3 or above display the same experimental electronic spectrum, which is reported in Figure 6, top. This spectrum shows a main characteristic band at λ_{max} = 650 nm, in coincidence with the reported spectra attributed to *p*-terphenyl dianion in solution.[16] To further characterize the compound responsible of this spectrum we performed a careful TDDFT simulation of the potential species involved, which include both loose and tight ionic pairs of the monoanion, dianion and trianion of *p*-terphenyl with solvated potassium as countercation, as in previous studies.[17] Preliminary results are unequivocal, only the dianion *p*-terphenyl^{-2} reproduces the pattern of a main absorption band near the experimental one, which corresponds to a $\pi \rightarrow \pi^*$ type of transition. Refined calculations, including two potassium ions solvated with DME in the model fit very well with the experimental spectrum (Figure 6, top). As seen in other experimental complexes,[18] the potassium cations in DME prefers adopting a squared antiprism octacoordination sphere with the eight oxygens of four DME molecules. This $K^+(DME)_4$ configuration is also well reproduced in our calculations, leading to the optimized complex $[K^+(DME)_4]_2$ [*p*-terphenyl^{-2}] of C_i symmetry (Figure 6, bottom). In this figure, the main electronic transition S_5 (A_u) of this complex is drawn, as well as the natural transition orbitals

---

[16] Former UV-vis studies of *p*-terphenyl mono and dianions in solution are described in the literature: A. Sakamoto, T. Harada, N. Tonegawa, A New Approach to the Spectral Study of Unstable Radicals and Ions in Solution by the Use of an Inert Gas Glovebox System: Observation and Analysis of the Infrared Spectra of the Radical Anion and Dianion of p-Terphenyl, *J. Phys. Chem. A* **2008**, *112*, 1180-1187.

[17] S. V. Bondarchuk, M. Carrera, M. de la Viuda, A. Guijarro, Spontaneous disproportionation of lithium biphenyl in solution: a combined experimental and theoretical study, *New J. Chem.*, **2018**, *42*, 5168-5177.

[18] See for instance cif in: B. Gehrhus, P. B. Hitchcock, R. Pongtavornpinyo, L. Zhang, Insights into the making of a stable silylene, *Dalton Trans.* **2006**, 1847-1857.

(NTO) representing the best hole/particle picture of the excited state.[19] This intense main transition is assigned as ψ_{280} (A_u) → ψ_{306} (A_g) (41%); ψ_{280} (A_u) → ψ_{304} (A_g) (−39%); ψ_{280} (A_u) → ψ_{301} (A_g) (−32%); ψ_{280} (A_u) → ψ_{294} (A_g) (−20%), and roughly matches the main intense S_5 (B_{1u}) transition obtained for the bare dianion *p*-terphenyl^{-2} of D_{2h} symmetry, assigned as ψ_{62} (B_{3u}) → ψ_{68} (B_{2g}), corresponding to the HOMO → LUMO+5 excitation. All TDDFT calculations were done at the wB97XD/6-311++G(2d,2p) level of theory in DME as simulated solvent. The assignment of the most important bands of the electronic spectrum for the bare dianion and solvated dipotassium complex can be found in the SI.

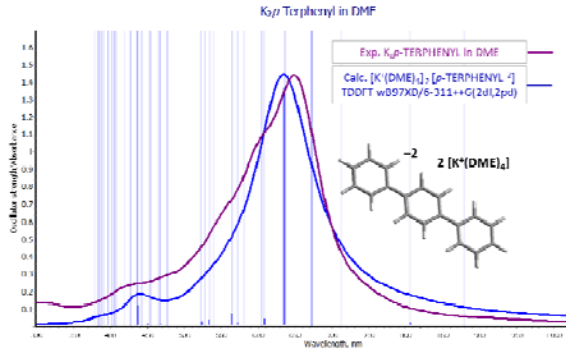

[19] Martin, R. L. Natural transition orbitals, *J. Chem. Phys.* **2003**, *118*, 4775-4777.

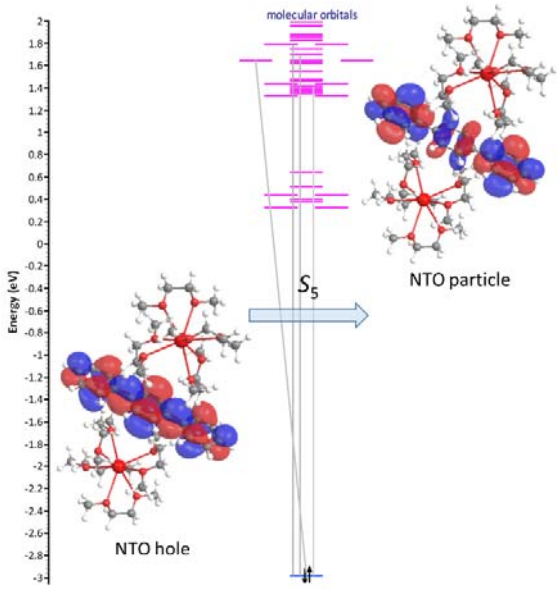

Figure 6. On the top, the experimental UV-vis spectra of K_xTp, for x≥2 in DME solution (magenta line, λ_{max} = 650 nm), superimposed to the TDDFT calculated spectrum of solvated Tp dianion $[K^+(DME)_4]_2$ [*p*-TERPHENYL^{-2}] (blue thick line) and individual transitions (blue thin vertical lines). All the black powders with formal composition K_xTp, x≥2 afford the same UV-vis spectra when dissolved in DME. On the bottom, the calculated electronic densities of hole and particle NTO pair corresponding to the main S_5 (A_u) dipole-allowed singlet excited state of this complex, as well as a diagram of the MOs transitions which are involved in the excited state.

6. MAGNETIC PROPERTIES OF K_xTp AND K_xPPP SAMPLES

We have measured the magnetic properties of all the intercalated materials studied above, as well as some synthetic variations under different conditions, such as annealing temperature, inert solvent, use of pressure and other metals. Table 1 summarizes all the materials studied and the experimental conditions under which they were synthesized.

Table 1. Intercalated materials submitted to magnetic behavior study. Meissner effect was absent in all cases.

Entry	Compound	*T* (ºC)	*t* (h)	notes
1	K_2Tp	100	72	
2	K_2Tp	180	62	
3	K_3Tp	100	39	
4	K_3Tp	180	62	pre-heated[a]
5	K_3Tp	180	48	pressure[b]
6	K_3Tp	250	39	
7	K_3Tp	250	70	
8	Cs_3Tp	25	72	in solution[c]
9	$[K(C_6H_4)_3]_n$	180	72	linear[d]
10	$[K(C_6H_4)_2]_n$	120	24	[d]
11	$[K_2(C_6H_4)_3]_n$	120	72	[d]
12	$[K(C_6H_4)]_n$	180	72	[d]
13	$[K_2(C_6H_4)]_n$	180	72	[d]
14	$[K(C_6H_4)_2]_n$	180	72	branched[e]
15	$[K_{0.9}(C_6H_4)_2]_n$	180	72	[e]
16	$[K_{1.1}(C_6H_4)_2]_n$	180	72	[e]

[a] Reaction of pre-heated reactants at the given T. [b] Annelation under pressure (ca. 1 GPa). [c] Reaction in benzene, removed after completion under high vacuum. [d] With linear PPP. [e] With branched PPP.

For *p*-terphenyl compounds, both K_2Tp and K_3Tp stoichiometries have been tested under mild and harsh annealing conditions (entries 1-7). In entry 4, instead of gradual heating of the mixed reactants, the reaction was carried out with the pre-heated reactants at the target *T* in an attempt to gain access to potential thermodynamically less stable minor phases. We turned then to the effect of pressure. A sample of K_3Tp stoichiometry was prepared under pressure by annealing inside a stainless steel screw press at *ca*. 1 GPa for two days (entry 5). The effect of alkali metals

more electropositive than K was also studied. The reaction with Cs occurs smoothly in benzene solution at room temperature until complete consumption of dissolved Tp takes place. The solvent was removed afterwards under high vacuum (10^{-4} Torr) up to constant weight. In a typical experiment, the temperature dependence of the magnetization of the sample *M* was recorded against temperature *T* in the presence of a small constant magnetic field (20-100 Oe) in field cooling runs (FC, more specifically FCC or field cooled cooling runs), or in the absence of magnetic field in zero-field cooling runs (ZFC). In Figure 7 we find a representative example of our results. It corresponds to the *M*/*T* plot of a sample of K_3Tp annealed at 250ºC (entry 7). The overall magnetic moment is positive, apparently due to the dominance of a paramagnetic background signal. Under cooling, there is a relatively flat, smooth dependence of *M* with the temperature which turns into a Curie-like behavior in the proximity of 0K. Still, we have found no signs of superconducting transition in either FC or ZFC modes from 100 to 20 Oe. The isothermal *M* against *H* plots (Figure 7, bottom) exhibit a magnetization hysteresis loop consistent with a weakly ferromagnetic background. Zooming in the *M*/*H* origin shows no signs of a diamagnetic response either, confirming the absence of a superconducting phase (insert).

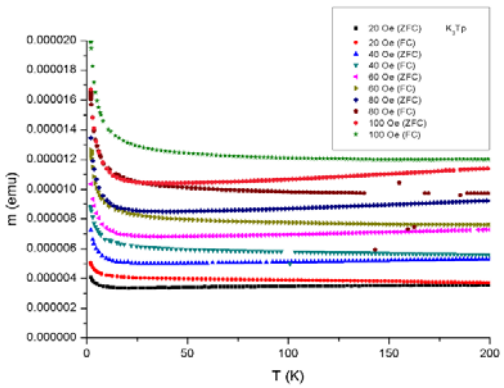

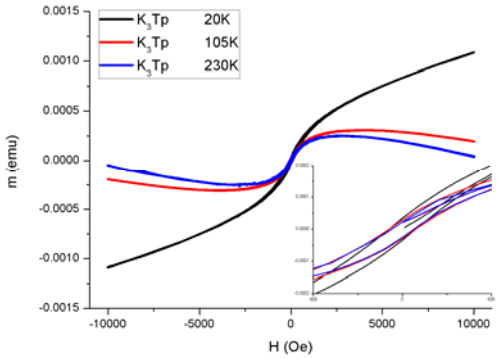

Figure 7. On top, K_3Tp annealed at 250ºC displays no apparent signs of Meissner effect in the plots *M vs. T* (top), and behaves in a similar manner in the plots *M vs. H* at different temperatures (bottom). The insert is a zoom around the *M*-*H* origin.

For the PPP series, the overall scenario found is not very different. Both Yamamoto's linear PPP,[9] and Kovacik's branched one,[10] were tested. Just like in the Raman studies, we have evaluated samples with stoichiometric mixing ratios of (p-C_6H_4)/K = 3/1, 2/1, 3/2 and 1/1 (entries 9-13), as well as quasi-stoichiometric, near the upper experimental K upload limit of 2/1, such as 2/0.9 and 2/1.1 (entries 14-16). We have selected in Figure 8, top, a representative example of the behavior of the doped PPP series. It corresponds to the *M*/*T* plot of substoichiometric $[K_{0.9}(C_6H_4)_2]_n$ (entry 15, Table 1), displaying again no apparent signs of Meissner effect in either the FC or ZFC runs from 100 to 20 Oe. In the bottom, plots of *M*/*H* at 20 K of lineal K_xPPP of increasing potassium mixing stoichiometries (entries 9-13 in Table 1) are shown, with the same outcome.

Expected small differences between FC and ZFC runs in all samples are likely due to a macroscopic texture of the materials, submitted to magnetometer analysis as a compacted pellet of the raw powder materials synthesized as described in Table 1. It is remarkable the similarity of the plots obtained for the Tp and PPP series of intercalated compounds.

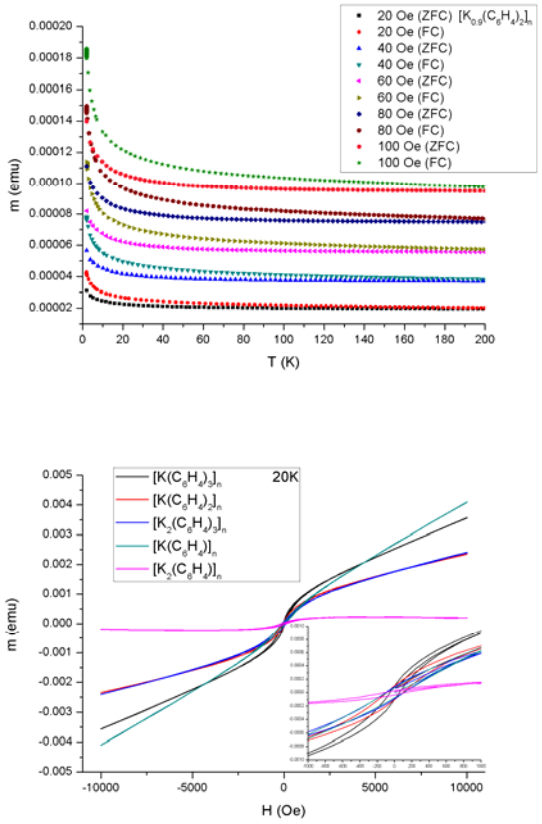

Figure 8. On top, as a representative example of the K_xPPP series, substoichiometric branched $[K_{0.9}(C_6H_4)_2]_n$ displaying no apparent signs of Meissner effect in the plots *M vs. T* (top). In the bottom, lineal K_xPPP of increasing potassium mixing stoichiometries behave in a similar manner (plots *M vs. H* at 20 K). The insert is a zoom around the *M*-*H* origin.

7. ELECTRICAL CONDUCTION PROPERTIES OF K_xTp

Finally, we have investigated the temperature dependence of the electrical resistivity ρ of some K_xTp samples in searching for a zero-resistivity signature. Figure 9 displays the experimental resistance versus temperature plot of a mildly annealed K_3Tp sample (180ºC, blue line). The graph displays a linear decrease of the resistivity of the sample with *T* in the high-temperature regime, $\rho(T) \propto T$, followed by power law of dependence when approaching zero K, $\rho(T) \propto T^n$ at

the low temperature regime. This is in accordance with the Bloch–Grüneisen treatment of conducting electrons in a metallic phase (fitting orange line), and describes our actual sample as a metal. While this behavior is difficult to be attributed either to an excess of potassium in a K_2Tp matrix or to a more complex composite type of material, the distinctive feature of a superconductive phase was not observed. Mildly or harshly annealed samples down to 4 K also fail to show a characteristic superconducting step. On the other hand, as expected from a band insulator, K_2Tp samples behaved always as insulators in our ρ/T determinations.

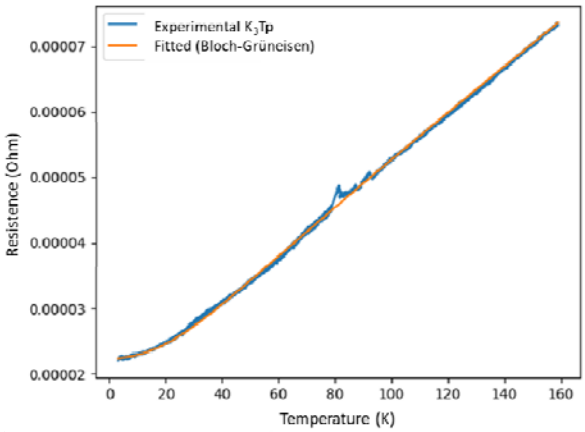

Figure 9. Temperature dependence of the electrical resistance of a K_3Tp pellet down to 4 K (blue line), and fitting to the Bloch-Grüneisen equation (in orange) confirming a metallic behavior (orange line). No signs of a superconducting transition were detected.

8. CONCLUSSIONS

We have carried out an extensive study of the K_xTp system as well as its polymeric extended congener K_xPPP regarding structural characterization and displayed magnetic/conductive properties. The structural integrity of Tp after K intercalation and different annealing conditions has been examined. The main phase of the different K_xTp mixtures obtained under mild conditions seems to be K_2Tp by Raman as well as UV-vis spectroscopy. Harsher reaction conditions and extended reaction times produce a matrix of insoluble byproducts, likely by

polymerization, so the potential role of PPP was incorporated into the study. Both linear as well as branched PPP intercalated with K were synthesized and characterized, establishing a doping limit in one K atom per every two phenylene units (*p*-C_6H_4). The characterization of the physical properties of different stoichiometries and preparations of K_xTp and K_xPPP reveals many similarities in the overall behavior of these materials. The most significant is that neither the K_xTp nor the K_xPPP series gave rise to a detectable diamagnetic response in *M/T* or a zero resistivity step in ρ/T plots consistent with the presence of a superconductor phase. This is in contrast with the reported superconducting properties of K_3Tp,[1-4] and the subsequent wave of higher oligomers reported thereafter describing similar performances under magnetic measurements, such as *p*-quaterphenyl,[20] and *p*-quinquephenyl.[21]

9. EXPERIMENTAL

p-Terphenyl (≥99.5%, Sigma-Aldrich), potassium (99.5%, cubes in mineral oil, Aldrich) and cesium (≥99.5%, Sigma-Aldrich) were used from our store without further purification. The rest of reagents used for the synthesis of PPP were commercially available (Merck, Alfa Aesar). Dry solvents (cyclohexane, DME) were distilled from K_2Na alloy under Ar atmosphere. Air sensitive manipulations were done using Schlenk techniques and/or glove bags under Ar purified through powdered KC_8. Annealing was done in a Pyrex tube either a) under dry Ar atmosphere, or b) under high vacuum conditions (10^{-4} Torr), using glass-coated magnetic stir bars for an efficient

[20] J.-F. Yan, G.-H. Zhong, R.-S. Wang, K. Zhang, H.-q. Lin, and X.-J. Chen, Superconductivity and Phase Stability of Potassium-Intercalated p-Quaterphenyl, *J. Phys. Chem. Lett.*, Just Accepted Manuscript, DOI: 10.1021/acs.jpclett.8b03263.

[21] G. Huang, G.-H. Zhong, R.-S. Wang, J.-X. Han, H.-Q. Lin, X.-J. Chen, Superconductivity and phase stability of potassium-doped p-quinquephenyl, *Carbon*, **2019**, 143, 837-843.

mixing. Alternatively, the reaction with K can be done in an inert solvent (freshly distilled dry cyclohexane at 70ºC) to ensure a full homogeneity of the final sample. There are no noticeable differences in the Raman spectra between these two dry and wet procedures after careful solvent removal. Similarly, Cs/benzene was used as a reaction media for room temperature synthesis. Quantification of the recovered Tp was done by exposition to air until the black color was quenched, addition of an internal standard (durene), extraction (hexane) and gas-liquid chromatography analysis (GLC HP-4890 equipped with a FID detector and a 30 m HP-5 capillary column) using a calibration curve. In parallel, the same samples were also quantitatively analyzed by 300 MHz ^{1}H NMR (Bruker AV-300) corroborating the GLC. measurements. Mass spectra by electronic impact (EI, 70 eV) were recorded using a direct insertion probe (DIP) (Agilent Network 5973). Raman spectra (Jasco NRS-5100) were recorded on powder samples inside a sealed capillary (2 mm ø) under Ar using excitation wavelengths of 532 and 633 nm at ca. 0.4 mW of laser power. Alternatively spectra at 785 and 1064 nm (FT-Raman Bruker RFS/100) were also checked, providing no better results. All the samples were homogeneous by Raman microscopic mapping (0.04 μm step). UV-vis spectra were recorded on a double beam spectrophotometer (Shimadzu UV-1603). Magnetic measurements were performed in compacted cylindrical pellets (ca. 4 mm ø x 5 mm) under He using a SQUID magnetometer (Quantum Design MPMS-55). Electrical resistance measurements were done using a 4 point probe on a compacted disk of material (10 mm ø x 2 mm) under Ar in a home-made steel cylindrical holder, using an electrical current source (Keithley 6221 DC-AC), a nanovoltmeter (Keithley 2182A), a temperature controller (Cryocon 32B) and liquid N_2 and He

as the cooling media. Density functional theory (DFT) calculations were performed using the Gaussian 09 suite of programs.[22]

AUTHOR INFORMATION

Corresponding Author

*Fax: (+34) 965-90-35-49. E-mail: aguijarro@ua.es

Notes

The contents of this work have been presented in the 12th Conference on Materials and Mechanisms of Superconductivity (M2S-HTSC-XII), Aug. 19-24, 2018, Beiging, China.

ASSOCIATED CONTENT

Supporting Information. Computational details data of the DFT Raman and TDDFT Uv-vis simulations of spectra.

ACKNOWLEDGEMENTS

Financial support by the Spanish Ministry of Economy and Competitiveness (FIS2015-64222-C2-1-P, MAT2014-52405-C2-2-R and MAT2016-78625-C2-1-2-P), the Generalitat Valenciana (Grant PROMETEO/2017/139) and the University of Alicante (VIGROB-285) is gratefully acknowledged. MC thanks the VIDI of the University of Alicante for a predoctoral grant. AG greatly appreciates the computational resources provided by the Department of Applied Physics of the University of Alicante.

---

[22] M. J. Frisch, G. W. Trucks, H. B. Schlegel, G. E. Scuseria, M. A. Robb, J. R. Cheeseman, G. Scalmani, V. Barone, B. Mennucci and G. A. Petersson, et al., Gaussian 09, Revision A.02, Gaussian, Inc., Wallingford, CT, 2009.

REFERENCES